NJC

RSC Publishing

PAPER

View Article Online
View Journal | View Issue

Luminescent carbon quantum dots and their application in cell imaging

Cite this: *New J. Chem.*, 2013, **37**, 2515

Hui Ding,[a] Li-Wei Cheng,[b] Ying-Ying Ma,[a] Ji-Lie Kong*[b] and Huan-Ming Xiong*[a]

Received (in Montpellier, France) 9th April 2013,
Accepted 28th May 2013

DOI: 10.1039/c3nj00366c

www.rsc.org/njc

A facile hydrothermal method was used to synthesize luminescent carbon dots from single-walled carbon nanotubes (SWNTs). Then 4,7,10-trioxa-1,13-tridecanediamine (TTDDA) was grafted onto the carbon dots to increase their water solubility and luminescent properties. The as-prepared carbon dots were characterized by UV-Vis absorption, infrared (IR), Raman, fluorescence, and transmission electron microscopy (TEM). The results confirmed that these carbon dots were monodispersed in water and emitted bright yellow fluorescence. The surface modified carbon dots were used to label biological cells, and the images obtained by a laser scanning confocal microscope showed that the carbon dots were gradually taken up by HeLa cells. The cytotoxicity of such carbon dots toward HeLa cells was very low, for 24 h the LC_{50} was over 5 mg mL^{-1}.

Published on 14 June 2013. Downloaded by Fudan University on 30/07/2013 04:01:50.

1 Introduction

Luminescent semiconductor quantum dots have aroused intensive attention due to their unique optical properties and promising biomedical applications.[1–5] However, typical QDs contain heavy metals as necessary elements, which bring severe disease to human beings and damage to the environment.[6,7] Hence, nontoxic and benign quantum dots with similar optical properties are required for practical applications. Luminescent carbon dots were first obtained during the purification of single-walled carbon nanotubes through electrophoresis in 2004.[8] Since then, various techniques have been employed to prepare carbon dots, including arc discharge,[8] laser ablation,[9–12] pyrolysis,[13,14] electrochemical synthesis,[15–20] template-supported synthesis,[21–23] acid oxidation,[24–26] microwave-assisted synthesis,[27–30] hydrothermal synthesis[31] and wet chemistry methods.[32–36] Carbon dots possess distinct advantages over organic dyes and many other semiconductor nanoparticles, such as high aqueous solubility, strong chemical inertness, good optical stability, facile functionalization, low cytotoxicity and excellent biocompatibility.[27,31,37–40] In several latest reports, carbon dots have exhibited emission in the near-infrared (NIR) spectra region, which is important for *in vivo* nanotechnology because the animal body is almost transparent in the NIR windows.[27,40,41] However, the quantum yield (QY) of carbon dots is usually very low, especially in the NIR windows. In addition, the photoluminescent mechanism of carbon dots remains unclear and controversial, which limits the improvement of the luminescent properties. Furthermore, most of the reported carbon dots mainly emit blue-green fluorescence, which could be covered by the autofluorescence of the cells and tissues. Therefore, carbon dots emitting yellow-red or NIR light with high QY are desired for bioimaging applications.

In the present research, we synthesized uniform monodispersed carbon dots through an acidolysis treatment on SWNTs under hydrothermal conditions. We found that the luminescent performances of the carbon dots could be enhanced by passivation of some amines, so we used TTDDA to increase the fluorescent intensity and water solubility of the carbon dots. The as-prepared solutions were transparent and stable, and emitted yellow fluorescence under a UV lamp. Afterwards, we used such luminescent carbon dots to label HeLa cells and study the uptake process under a confocal microscope.

2 Experimental section

2.1 Synthesis of TTDDA modified carbon dots

50 mg of SWNTs (carbon > 90 wt%, Aldrich) was added to a mixture solution of nitric acid (65 wt%, 5 ml) and high chlorine acid (70 wt%, 5 ml). The mixture was sonicated for 10 min, and then transferred to a polytetrafluoroethylene-lined stainless steel autoclave for 24 h reaction at 100 °C. Afterwards, the reaction mixture was cooled to room temperature and 50 ml of deionized water was added. A sintered glass funnel, with a pore

[a] *Department of Chemistry and Shanghai Key Laboratory of Molecular Catalysis and Innovative Materials, Fudan University, Shanghai 200433, P. R. China. E-mail: hmxiong@fudan.edu.cn*

[b] *Department of Chemistry and Institutes of Biomedical Sciences, Fudan University, Shanghai, 200433, P. R. China. E-mail: jlkong@fudan.edu.cn*

Published on 14 June 2013. Downloaded by Fudan University on 30/07/2013 04:01:50.

size of about 0.1 μm, was used to filter the mixture and the obtained red brown solution was placed in a dialysis bag (M. W. cutoff 3500, Spectrum). The solution was dialyzed against deionized water for 3 days. Later, 20 ml of the dialyzed solution was mixed with 0.1 g of Na_2HPO_4 and 0.5 g of TTDDA (Aldrich) in a polytetrafluoroethylene-lined stainless steel autoclave and heated to 180 °C for 12 h. After cooling to room temperature, the solution was dialyzed against deionized water for another 3 days.

2.2 Characterization

A JEM-2010 transmission electron microscope operating at 200 kV was employed to obtain high resolution transmission electron microscopy (HRTEM) images. The Raman spectrum of the as-prepared samples was recorded by a LabRam-1B micro Raman spectrometer. Fourier transform infrared (FT-IR) spectra were recorded on a Nicolet Nexus 470 FT-IR Spectrometer. The UV-Vis absorption spectra were recorded on a Unico UV-2802 PC spectrometer. The photoluminescence (PL) spectra were measured by a Horiba JobinYvon fluoromax-4 spectrofluorometer equipped with a HORIB-F-3004 sample heater/cooler Peltierthermocouple drive and an F-3018 quantum yield accessory including an integrating sphere. For the heating scan, the carbon dot aqueous solution was freeze-dried and then dispersed in triethylene glycol. A photostability comparison between a carbon dot solution and a Rhodamine-6G solution with their optical densities below 0.1 was conducted by continuous irradiation under a UV lamp. After irradiation for different lengths of time, the fluorescent intensity of the samples were measured on the fluorescence spectrometer under the same conditions.

For the cellular toxicity test, HeLa cells were seeded into a 96-well cell culture plate in DEME at a density of 10^4 cells per ml with 5% fetal bovine serum at 37 °C and with 5% CO_2 for 24 h. Afterwards, the culture medium was replaced with 100 μL of DMEM containing the carbon dots at different doses and cultured for another 24 h. Then, 20 μL of 5 mg mL^{-1} MTT (3-(4,5-dimethylthiazol-2yl)-2,5-diphenyltetrazolium bromide) solution was added to every cell well. The cells were further incubated for 4 h, followed by removing the culture medium with MTT, and then 100 μL of DMSO was added. The resulting mixture was shaken for 10 min at room temperature. The absorbance of MTT at 492 nm was measured by an automatic ELISA analyzer (SPR-960). The control data was obtained in the absence of carbon dots. Each experiment was performed 5 times and the average data was presented. Cellular fluorescent images were recorded on a Leica TCS SP5 Laser Scanning Confocal Microscope. HeLa cells were seeded on cover slips in the cell culture DMEM for 1 day. The medium was then mixed with carbon dots for imaging at different times. Excitation of the samples was performed by a laser of λ = 476 nm, and emission was recorded in the range from 550 nm to 600 nm.

3 Results and discussion

The TEM image (left) in Fig. 1 shows that the carbon dots are monodispersed and homogeneous, with an average diameter of about 4 nm. The HRTEM (right) image of the carbon dots reveals a lattice spacing of 0.32 nm, which is in accordance with nanoparticles derived from graphite by other researchers.[15] Since our product is made from SWNTs, its uniformity and purity can be expected.

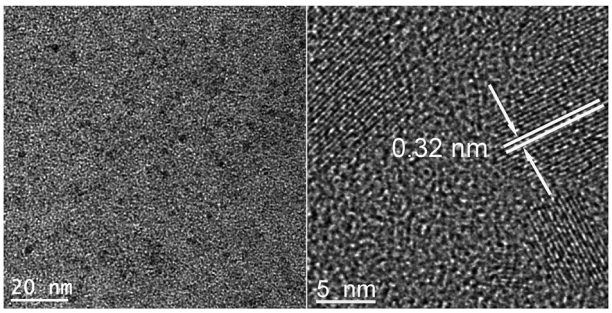

Fig. 1 TEM (left) and HRTEM (right) images of the carbon dots.

In Fig. 2, the Raman spectrum of the carbon dots exhibits two peaks at 1352 and 1582 cm^{-1}, corresponding to the D and G bands of carbon, respectively. The ratio of I_D/I_G is 1.384, which is characteristic of the disorder extent and the ratio of sp^3/sp^2 carbon,[42] implying that structural defects are introduced into the nanoparticles after oxidation.

A FT-IR technique was used to identify the organic functional groups on the surface of the carbon dots. As shown in Fig. 3, there are two new bands of the carbon dots, 1714 and 1400 cm^{-1}, that are attributed to the C═O and C–N bands, respectively, which indicates the formation of amide groups after passivation. IR bands of the carbon dots at 1593 and 1574 cm^{-1} represent the bending vibration of the N–H bonds. Both samples have absorptions at about 3400 and 1100 cm^{-1}, which are ascribed to N–H asymmetric stretching and C–O stretching vibrations, respectively. According to the above analyses, TTDDA groups have been modified onto the carbon dots through covalent bonds. Such covalent bonds are believed to result from the reaction between the amine groups of TTDDA and the carboxyl groups on the surface of the carbon dots. It has been reported that the carboxyl groups on the surface of the carbon dots were from the acid oxidation, which contribute to

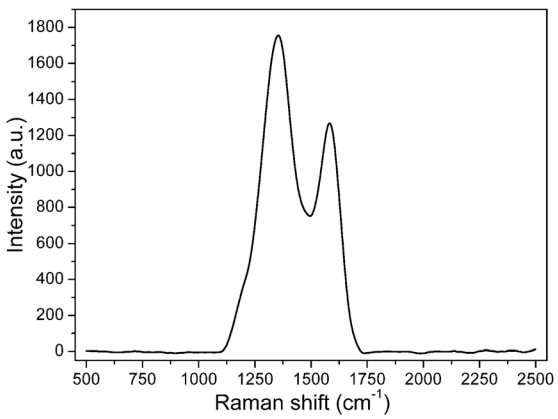

Fig. 2 Raman spectrum of the carbon dots (excitation wavelength: 632.8 nm).

 This journal is © The Royal Society of Chemistry and the Centre National de la Recherche Scientifique 2013

Published on 14 June 2013. Downloaded by Fudan University on 30/07/2013 04:01:50.

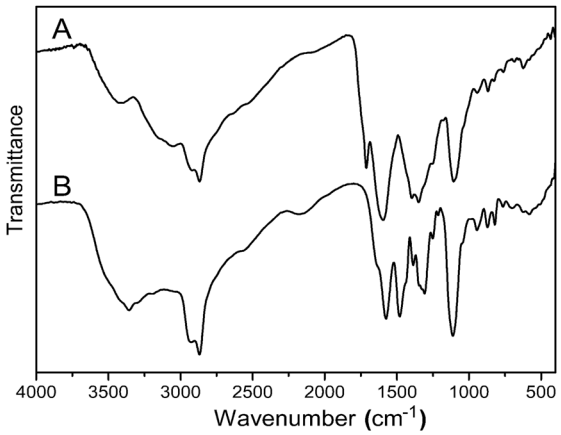

Fig. 3 FT-IR spectra of (A) carbon dots modified with TTDDA, and (B) TTDDA itself.

the weak luminescence of the carbon dots.[25] Hence, passivation by TTDDA is able to improve the luminescent properties and water solubility of the carbon dots simultaneously.

The UV-Vis absorbance curve of the as-prepared carbon dots in Fig. 4 shows a broad absorption range with typical $\pi \rightarrow \pi^*$ transition bands in the UV region. According to previous research,[42] such a broad absorption can be ascribed to the complicated band structure and random energy levels of the carbon dots. It is interesting that the PL emission is centered around 600 nm when we use different excitation light ranging from 350 to 550 nm. The PL emission spectra exhibits a red shift with the increment of the excitation wavelength. When the excitation wavelength is 470 nm, our carbon dots show the strongest fluorescence. The yellow fluorescence of the carbon dots in water under UV light is shown in the inset of Fig. 4. In many previous reports,[27–30] the PL emissions of the carbon dots were mainly blue, while the yellow or red emissions were very weak. However, for practical bioimaging, PL emission with a longer wavelength is preferred because the cell nuclei usually emit blue light. Thus, our product is more suitable for cell imaging.

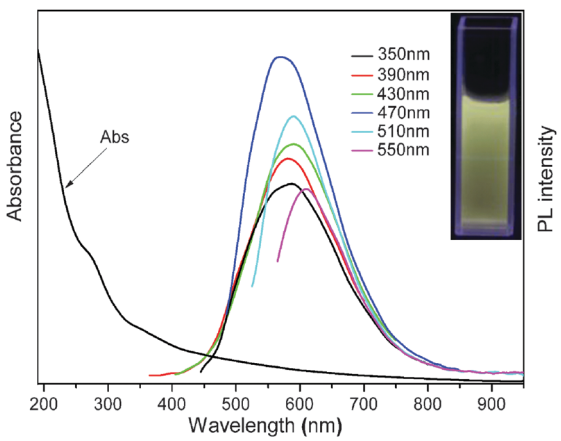

Fig. 4 UV-Vis absorption spectra (Abs) and PL emission spectra of the surface-passivated carbon dots in water obtained by excitation wavelengths from 350 to 550 nm. The inset picture is the same sample under a UV lamp.

A sufficient quantum yield of a fluorescent probe is required for cell imaging. The evaluation of the quantum yield usually uses a traditional method that compares the emission of a reference and sample,[30] which possesses considerable error. Here we use an integrating sphere to directly measure the quantum yield of our sample. The sample is placed in an integrating sphere, and is excited by monochromatic light. The sample absorbance A is calculated by

$$A = \frac{L_b - L_c}{L_b} \quad (1)$$

where L_b is the integrated excitation profile when the sample is diffusely illuminated by the integrating sphere's surface, and L_c is the integrated excitation profile when the sample is directly excited by the incident beam.

The quantum yield Φ is, by definition, the emitted photons divided by the absorbed photons,

$$\Phi = \frac{E_c - (1 - A)E_b}{L_a A} = \frac{E_c - E_a}{L_a - L_c} \quad (2)$$

where E_c is the integrated luminescence of the sample caused by direct excitation, and E_b is the integrated luminescence of the sample caused by indirect illumination from the sphere. L_a is the integrated excitation profile from an empty integrating sphere (*i.e.*, without any sample), and E_a is the integrated luminescence from an empty integrating sphere (only as a blank). For integration of function L over the wavelength λ, the integration limits can be from 10 nm below the excitation wavelength to 10 nm above the excitation wavelength. The quantum yield of the final product was evaluated to be 4.5% by using the integrating sphere, which was higher than that of the carbon dots before passivation (QY = 2.3%).

In order to investigate the fluorescence property of the carbon dots, we tested the PL intensity with the change of temperature. It was found that the PL intensity evidently decreases upon increasing temperature. The result is the same as for the performances of other carbon dots, which is attributed to thermally activated nonradiative trapping.[43] At low temperatures, the nonradiative channel is not thermally activated, so the excited electrons can radiatively emit photons. Once the temperature is increased, the nonradiative channels become thermally activated. The nonradiative lifetime decreases with increasing temperature, which could be expressed as

$$\tau_{NR} = \tau_0 \exp(E_a/K_B T) \quad (3)$$

where E_a denotes an activation energy, K_B is the Boltzmann constant.

In a steady state, since PL intensities are proportional to n/τ_R, the following familiar expression is obtained.

$$I(T) = I_0/[1 + (\tau_R/\tau_0)\exp(-E_a/K_B T)] \quad (4)$$

where τ_R is the radiative lifetimes.[43] This formula matches well with our results shown in Fig. 5.

One important advantage of carbon dots over traditional dyes as fluorescent labels is their better photostability. In the photobleaching measurements in Fig. 6, the fluorescence

Published on 14 June 2013. Downloaded by Fudan University on 30/07/2013 04:01:50.

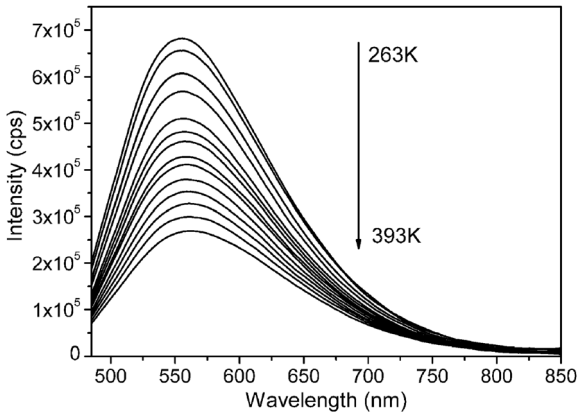

Fig. 5 PL emission spectra of the carbon dots in triethylene glycol solution at different temperatures. The temperature increment step is 10 K.

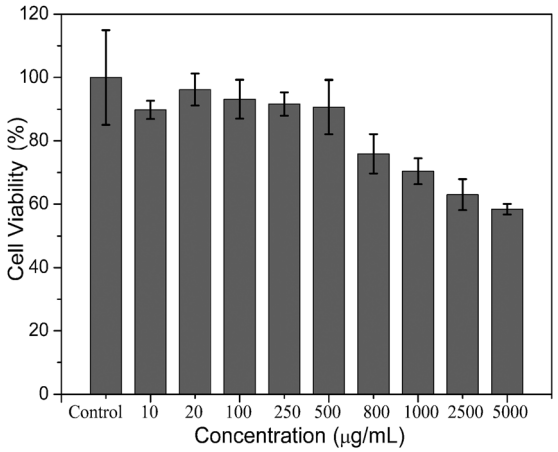

Fig. 7 Cytotoxicity of the carbon dots toward HeLa cells from a MMT assay.

intensity of the carbon dots exhibited almost no change, while an obvious fluorescent decay was observed for R6G after 2 h of continuous UV irradiation. Hence, our carbon quantum dots are more stable than conventional dyes for cell imaging.

Low cytotoxicity is one of the most critical requirements for ideal multifunctional biomaterials with bioimaging capacity. Hence, we used a MTT assay method to evaluate the cytotoxicity of the carbon dots. After incubation with HeLa cells for 24 h, the MTT results (Fig. 7) showed that the carbon dots exhibited very low cytotoxicity. Cell viability was over 90% when the concentration of the carbon dots is below 500 μg mL^{-1}. Even when the concentration was up to 5 mg mL^{-1}, the cells retaining viability was about 58%, which was better than many other reports. For example, in the work of Liu *et al.*, carbon dots had serious cytotoxicity when the concentration was up to 400 μg ml^{-1}.[44] Hence, the TTDDA-modified carbon dots showed very good compatibility with biological cells.

Since our carbon dots have very low cytotoxicity, they can also be used as bioimaging probes. After incubation with HeLa cells for 24 h, the carbon dots were uptaken by HeLa cells and the cells were alive under confocal microscopy (Fig. 8a). The carbon dots mainly existed in the cytoplasm and emitted yellow fluorescence, while the nuclei were not luminescent (Fig. 8b).

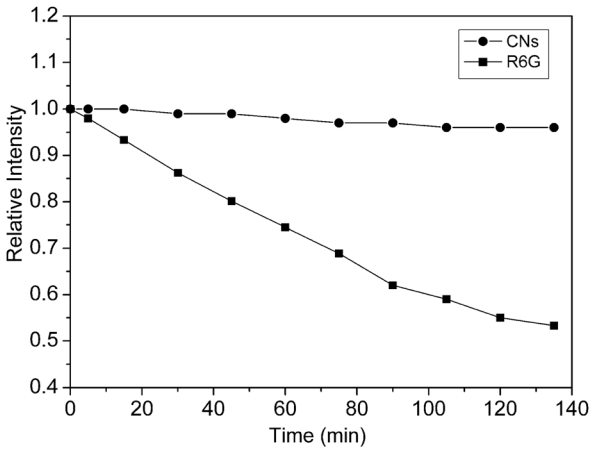

Fig. 6 Dependence of fluorescence intensity on UV irradiation time for CDs and a traditional dye (Rhodamine 6G). The relative intensity is the ratio value between the emission maximum of the irradiated samples and that of the original sample.

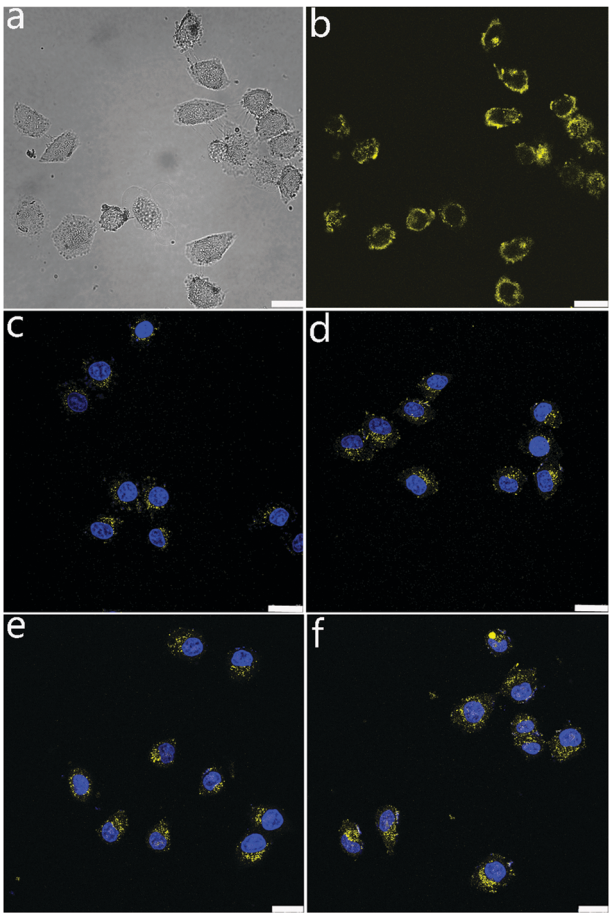

Fig. 8 Confocal luminescence images of HeLa cells incubated with 1 mg mL^{-1} of CNs-TTDDA. (a) The DIC image for HeLa cells after 24 h incubation, (b) the fluorescent image of (a). After being marked by blue dye (4, 6-diamidino-2-phenylindole), the images of the cells were taken at different times: (c) 10 min, (d) 40 min, (e) 120 min and (f) 360 min. The bar in each picture represents 25 μm.

 This journal is © The Royal Society of Chemistry and the Centre National de la Recherche Scientifique 2013

Published on 14 June 2013. Downloaded by Fudan University on 30/07/2013 04:01:50.

In order to dynamically study the cell uptake, we marked the nuclei with blue dye (4′ 6-diamidino-2-phenylindole, DAPI), and incubated the cells with a culture containing carbon dots. From Fig. 8c to f, it is clear that more and more carbon dots penetrated the cells and located in the cytoplasm. This phenomena was similar to our previous study employing ZnO quantum dots.[45]

4 Conclusion

In summary, we have developed an efficient approach for synthesizing a new carbon dots fluorescence probe. The cytotoxicity of such a probe was very low, even when the concentration of carbon dots was up to 5 mg mL^{-1}. The cell imaging experiments proved that our carbon dots had a potential for biological applications. In addition, we studied the photoluminescence of such carbon dots at different temperatures, which helped to understand the luminescent mechanism of the carbon dots.

Acknowledgements

This work was supported by the National Basic Research Program of China (2013CB934101), the National Natural Science Foundation of China (20873029, 21175029, 21271045), the NCET-11-0115 and the Shanghai Leading Academic Discipline Project (B109).

Notes and references

1 X. Michalet, F. F. Pinaud, L. A. Bentolila, J. M. Tsay, S. Doose, J. J. Li, G. Sundaresan, A. M. Wu, S. S. Gambhir and S. Weiss, *Science*, 2005, **307**, 538.
2 X. H. Gao, Y. Y. Cui, R. M. Levenson, L. W. K. Chung and S. M. Nie, *Nat. Biotechnol.*, 2004, **22**, 969.
3 I. L. Medintz, H. T. Uyeda, E. R. Goldman and H. Mattoussi, *Nat. Mater.*, 2005, **4**, 435.
4 K. Sanderson, *Nature*, 2009, **459**, 760.
5 J. Jung, A. Solanki, K. A. Memoli, K. Kamei, H. Kim, M. A. Drahl, L. J. Williams, H. R. Tseng and K. B. Lee, *Angew. Chem., Int. Ed.*, 2010, **49**, 103.
6 A. M. Derfus, W. C. W. Chan and S. N. Bhatia, *Nano Lett.*, 2004, **4**, 11.
7 R. Hardman, *Environ. Health Perspect.*, 2006, **114**, 165.
8 X. Xu, R. Rey, Y. Gu, H. J. Ploehm, L. Gearheart, K. Raker and W. A. Scrivens, *J. Am. Chem. Soc.*, 2004, **126**, 12736.
9 L. Cao, X. Wang, M. J. Meziani, F. Lu, H. Wang, P. G. Luo, Y. Lin, B. A. Harruff, L. M. Veca, D. Murray, S. Y. Xie and Y. P. Sun, *J. Am. Chem. Soc.*, 2007, **129**, 11318.
10 S. T. Yang, L. Cao, P. G. Luo, F. S. Lu, X. Wang, H. F. Wang, M. J. Meziani, Y. F. Liu, G. Qi and Y. P. Sun, *J. Am. Chem. Soc.*, 2009, **131**, 11308.
11 S. T. Yang, X. Wang, H. Wang, F. Lu, P. G. Luo, L. Cao, M. J. Meziani, J. H. Liu, Y. Liu, M. Chen, Y. Huang and Y. P. Sun, *J. Phys. Chem. C*, 2009, **113**, 1810.
12 X. Wang, L. Cao, F. S. Lu, M. J. Meziani, H. Li, G. Qi, B. Zhou, B. A. Harruff, F. Kermarrec and Y. P. Sun, *Chem. Commun.*, 2009, 3774.
13 F. Wang, Z. Xie, H. Zhang, C. Y. Liu and Y. G. Zhang, *Adv. Funct. Mater.*, 2011, **21**, 1207.
14 H. Peng and J. Travas-Sejdic, *Chem. Mater.*, 2009, **21**, 5563.
15 H. T. Li, X. D. He, Z. H. Kang, H. Huang, Y. Liu, J. L. Liu, S. Y. Lian, C. H. A. Tsang, X. B. Yang and S. T. Lee, *Angew. Chem., Int. Ed.*, 2010, **49**, 4430.
16 H. Ming, Z. Ma, Y. Liu, K. M. Pan, H. Yu, F. Wang and Z. H. Kang, *Dalton Trans.*, 2012, **41**, 9526.
17 J. Lu, J. X. Yang, J. Wang, A. Lim, S. Wang and K. P. Loh, *ACS Nano*, 2009, **3**, 2367.
18 Q. L. Zhao, Z. L. Zhang, B. H. Huang, J. Peng, M. Zhang and D. W. Pang, *Chem. Commun.*, 2008, 5116.
19 L. Y. Zheng, Y. W. Chi, Y. Q. Dong, J. P. Lin and B. B. Wang, *J. Am. Chem. Soc.*, 2009, **131**, 4564.
20 J. G. Zhou, C. Booker, R. Y. Li, X. T. Zhou, T. K. Sham, X. L. Sun and Z. F. Ding, *J. Am. Chem. Soc.*, 2007, **129**, 744.
21 A. B. Bourlinos, A. Stassinopoulos, D. Anglos, R. Zboril, V. Georgakilas and E. P. Giannelis, *Chem. Mater.*, 2008, **20**, 4539.
22 R. L. Liu, D. Q. Wu, S. H. Liu, K. Koynov, W. Knoll and Q. Li, *Angew. Chem., Int. Ed.*, 2009, **48**, 4598.
23 J. Zong, Y. H. Zhu, X. L. Yang, J. H. Shen and C. Z. Li, *Chem. Commun.*, 2011, **47**, 764.
24 H. P. Liu, T. Ye and C. D. Mao, *Angew. Chem., Int. Ed.*, 2007, **46**, 6473.
25 Z. A. Qiao, Y. F. Wang, Y. Gao, H. W. Li, T. Y. Dai, Y. L. Liu and Q. S. Huo, *Chem. Commun.*, 2010, **46**, 8812.
26 H. Q. Tao, K. Yang, Z. Ma, J. M. Wan, Y. J. Zhang, Z. H. Kang and Z. Liu, *Small*, 2012, **8**, 281.
27 L. B. Tang, R. B. Ji, X. K. Cao, J. Y. Lin, H. X. Jiang, X. M. Li, K. S. Teng, C. M. Luk, S. J. Zeng, J. H. Hao and S. P. Lau, *ACS Nano*, 2012, **6**, 5102.
28 H. Zhu, X. L. Wang, Y. L. Li, Z. J. Wang, F. Yang and X. R. Yang, *Chem. Commun.*, 2009, 5118.
29 Q. L. Wang, H. Z. Zheng, Y. J. Long, L. Y. Zhang, M. Gao and W. J. Bai, *Carbon*, 2011, **49**, 3134.
30 X. H. Wang, K. G. Qu, B. L. Xu, J. S. Ren and X. G. Qu, *J. Mater. Chem.*, 2011, **21**, 2445.
31 A. B. Bourlinors, A. Stassinopoulos, D. Anglos, R. Zboril, M. Karakassides and E. P. Giannelis, *Small*, 2008, **4**, 455.
32 J. Wang, X. Xin and Z. Lin, *Nanoscale*, 2011, **3**, 3040.
33 X. Yan, X. Cui, B. S. Li and L. S. Li, *J. Am. Chem. Soc.*, 2010, **132**, 5944.
34 I. P. Hamilton, B. Li, X. Yan and L. S. Li, *Nano Lett.*, 2011, **11**, 1524.
35 L. S. Li and X. Yan, *J. Phys. Chem. Lett.*, 2010, **1**, 2572.
36 X. Yan, X. Cui and B. S. Li, *Nano Lett.*, 2010, **10**, 1869.
37 S. N. Baker and G. A. Baker, *Angew. Chem., Int. Ed.*, 2010, **49**, 6726.
38 J. H. Shen, Y. H. Zhu, X. L. Yang and C. Z. Li, *Chem. Commun.*, 2012, **48**, 3686.
39 S. C. Ray, A. Saha, N. R. Jana and R. Sarka, *J. Phys. Chem. C*, 2009, **113**, 18546.

40 H. T. Li, X. D. He, Y. Liu, H. Huang, S. Y. Lian, S. T. Lee and Z. H. Kang, *Carbon*, 2011, **49**, 605.
41 S. F. Lim, R. Riehn, W. S. Ryu, N. Khanarian, C. K. Tung, D. Tank and R. H. Austin, *Nano Lett.*, 2006, **6**, 169.
42 H. T. Li, Z. H. Kang, Y. Liu and S. T. Lee, *J. Mater. Chem.*, 2012, **22**, 24230.
43 P. Yu, X. M. Wen, Y. R. Toh and J. Tang, *J. Phys. Chem. C*, 2012, **116**, 25552.
44 C. J. Liu, P. Zhang, F. Tian, W. C. Li, F. Li and W. G. Liu, *J. Mater. Chem.*, 2011, **21**, 13163.
45 H. J. Zhang, X. M. Xiong, Q. G. Ren, Y. Y. Xia and J. L. Kong, *J. Mater. Chem.*, 2012, **22**, 13159.

Published on 14 June 2013. Downloaded by Fudan University on 30/07/2013 04:01:50.

 This journal is © The Royal Society of Chemistry and the Centre National de la Recherche Scientifique 2013